CO_2 solubility and mass transfer in water-lean solvents

Ricardo R. Wanderley[a,b], Ye Yuan[b], Gary T. Rochelle[b], Hanna K. Knuutila[a,*]

[a]Department of Chemical Engineering, Norwegian University of Science and Technology, 7491 Trondheim, Norway

[b]McKetta Department of Chemical Engineering, The University of Texas at Austin, 200 E Dean Keeton St., Austin, TX 78712, United States

Graphical abstract

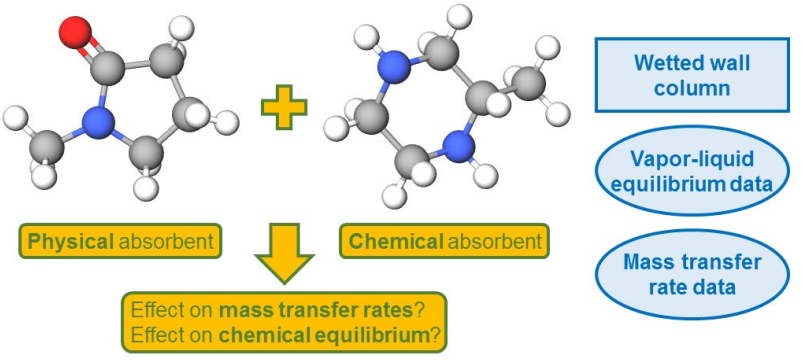

Abstract

Shifting from aqueous to water lean solvents has been evaluated as a mean for increasing the mass transfer rates in regular chemical solvents with amines. An array of amines (monoethanolamine, 2-methylpiperazine and N-methyl diethanolamine) and diluents (sulfolane, ethylene glycol, 1-methylimidazole, dimethyl sulfoxide, N-methyl-2-pyrrolidinone) has been analyzed. Addition of organic diluents seem to generally induce both a shift in chemical equilibrium and an increase in mass transfer rates for a fixed CO_2 partial pressure, though not necessarily for a fixed CO_2 loading. However, these relative advantages in terms of mass transfer rates decrease the more loaded the water lean solvent is. The equilibrium shift caused by organic diluents has been evaluated in terms of de-stabilization of the species in the solvent, which for monoethanolamine-based solvents can be easily related to a decrease in dielectric permittivity. However, this analysis indicates that such treatment is insufficient for other types of water-lean solvents, suggesting that different kinds of intermolecular interactions should also be considered in future studies.

*Keywords:*CO2 absorption, water lean solvents, hybrid solvents, mass transfer rates

1. Introduction

Amine scrubbing is currently the most mature technology for CO_2 sequestration (Bhown and Freeman, 2011). In the context of the biogas industry, it comes behind only water scrubbing as the preferred technical alternative for the upgrading to biomethane (IEA Bioenergy, 2016). Rendering amine scrubbing for biogas upgrading more competitive is important not only for economical purposes, but also for raising the attractiveness of biogas as a renewable source of energy.

* Corresponding author. Tel.: +47 73594119
E-mail address: hanna.knuutila@ntnu.no

In terms of operational expenditures (OPEX), amine scrubbing is one of the most expensive alternatives for biogas upgrading, demanding about 0.112 €/m^3 of biomethane in large capacity plants against the 0.091 €/m^3 required by water scrubbing plants. Their capital expenditures (CAPEX) are roughly the same (TUV, 2012). The advantage that this process displays over competing technologies rests upon its reliability and capacity for delivering high purity biomethane (TUV, 2012). As biomethane specifications are tightened and injection to the gas grid and production of liquefied biogas (LBG) becomes more common (Ryckebosch et al., 2011), fixing the issues with the energetic cost of amine scrubbing is a priority.

Water-lean solvents, or hybrid solvents, are a proposed alternative for the typical aqueous amine solvents employed in the industry. They consist of blends of amine and organic diluents and possess low or no water content. Research on this category of solvent has been going on for decades (Woertz, 1972; Semenova and Leites, 1977; Rivas and Prausnitz, 1979), though their popularity has resurfaced in the past few years (Lail et al., 2014; Yamamoto et al., 2014).

To be competitive, water-lean solvents have to perform better than the previous benchmarks for CO_2 capture, namely aqueous monoethanolamine (first generation solvents) and aqueous piperazine (second generation solvents) (Rochelle et al., 2011). Typically this comparison is made in terms of OPEX-related issues: it has been claimed that water lean solvents may possess higher capacity for CO_2 capture and lower regeneration energy penalties, as well as other advantageous physical properties (Yamamoto et al., 2014). However, little attention is paid on how mass transfer rates shift in water lean solvents in contrast with their aqueous counterparts.

Recent studies (Yuan and Rochelle, 2018) have shown how addition of organic diluents such as N-methyl-2-pyrrolidinone and sulfolane may promote the liquid-film mass transfer coefficients of ordinary amine solvents. This relates directly to the amount of packing required to perform the same operation and therefore to the CAPEX of the process, of which the absorber alone composes roughly 30% (Yuan and Rochelle, 2018). This opens another front on which to approach the issue of the viability of water lean solvents as alternatives for amine scrubbing technologies.

The present study expands the analysis made by previous researchers (Yuan and Rochelle, 2018) while focusing particularly on a series of proposed organic diluents and amines. The effects of adding organic diluents to chemical solvents, both in terms of shifts to CO_2 solubilities and mass transfer rates, have been investigated and exposed. This allows for some insights regarding the interplay of chemical properties in water-lean solvents. When possible, the observed phenomena have been directly correlated to such properties. Otherwise, a case-by-case analysis has been employed.

Symbols

a_i	activity coefficient of component i
A, B	respectively slope and intercept for linear regression between loadings and the logarithm of CO_2 equilibrium partial pressures
C_1-C_3	empirical coefficients for correlation with Hansen solubility parameters
D_i	diffusivity coefficient of component i
H_i	Henry's constant defined in terms of infinite dilution of component i in pure water
k_3	third order forward reaction rate constant between amine and CO_2
K_{eq}	equilibrium constant for the reaction between amine and CO_2
k_g	gas-film mass transfer coefficient
k_g'	liquid-film mass transfer coefficient
K_g	overall mass transfer coefficient
N_i	molar flux of CO_2 component i
p	pressure
p_i	partial pressure of component i
Q	molar flow rate
S	surface are of the stainless steel rod
x_i	concentration of component i
Δu	driving force for mass transfer
α	loading defined in terms of mol CO_2/mol N (e.g. each molecule of MEA has one reactive N site, whereas

	each molecule of 2MPZ has two.)
β_1, β_2	Respectively intercept and slope for linear regression necessary for obtaining the CO_2 partial pressure
δ	solubility parameter, specifically Hildebrandt solubility parameter if no subscript is given
γ_i	activity coefficient of component i
ε	dielectric permittivity
μ	dipole moment

Superscripts and subscripts

aq	relative to aqueous solvents
d	relative to London dispersion forces for Hansen solubility parameter
gas, b	relative to the bulk of the gas phase
h	relative to hydrogen bonding forces for Hansen solubility parameter
hyb	relative to hybrid solvents
in	relative to inlet, in the context of the wetted-wall column
int	relative to the interface between gas and liquid phases
out	relative to outlet, in the context of the wetted-wall column
liq, b	relative to the bulk of the liquid phase
p	relative to dipole-dipole forces for Hansen solubility parameter

2. Theory

2.1. Chemical equilibrium shift in water lean solvents

Chemical equilibrium in water lean solvents has been object of numerous studies (Alvarez-Fuster et al., 1981; Sada et al., 1985, 1986) and yet there is no consensus even on whether the diluent may take part in the reaction mechanism or not (Versteeg and van Swaaij, 1988). Nevertheless, it is clear that shifting the medium from aqueous to water-lean has effects on the conversion of amine and CO_2 to their ionic products. Typically this effect has been reported as a depression of both conversion and conversion rates (Sada et al., 1985, 1986).

This depression effect can be seen as a shift of the vapor-liquid equilibrium (VLE) curve to the left: for a fixed CO_2 partial pressure (p_{CO2}) in the vapor phase, the hybrid solvent in equilibrium contains lower CO_2 loading (α) than its aqueous equivalent. At low loadings and partial pressures, i.e. in situations wherein the solvent still has considerable stoichiometric capacity for absorbing and reacting with CO_2, these VLE curves may appear as parallel straight lines in a logarithmic plot. Previous studies (Yuan and Rochelle, 2018; Roberts and Mather, 1988; Kohl and Nielsen, 1997) show that this is valid only in a very limited interval. For higher loadings, one may even observe complete crossovers of VLE lines due to extended absorption capacities of water lean solvents (Roberts and Mather, 1988; Kohl and Nielsen, 1997). However, by focusing on the limited span where the lines seem to be parallel, one ends up with a convenient measure for evaluating water lean solvents: the magnitude of the left-leaning shift. Such a measure is developed in the following paragraphs, as well as its proposed physical meaning.

Equation (1) shows the simplest representation of the reaction between MEA and CO_2. At lower loadings, it is acceptable to neglect bicarbonate and/or carbonate formation as mechanisms of conversion for this interpretation.

$$CO_2^{(g)} + 2 \cdot MEA^{(l)} \xleftrightarrow{K_{eq}} MEACOO^{-(l)} + MEAH^{+(l)} \quad (1)$$

With K_{eq} described in terms of activities, its value will be the same for reactions in both aqueous and water lean solvents. The expression for K_{eq} is given in Equation (2). The value of Henry's coefficient, H_{CO2}, is defined in terms of its infinite dilution in pure water, so that it will be the same for both hybrid and aqueous solvents.

$$K_{eq} = \frac{a_{MEAH+} \cdot a_{MEACOO-}}{a_{MEA}^{2} \cdot a_{CO2}} = \frac{x_{MEAH+} \cdot x_{MEACOO-}}{x_{MEA}^{2}} \cdot \frac{\gamma_{MEAH+} \cdot \gamma_{MEACOO-}}{\gamma_{MEA}^{2}} \cdot \frac{H_{CO2}}{p_{CO2}} \quad (2)$$

With Equation (2), it becomes clear that, at fixed α, the ratio between p_{CO2} in hybrid and aqueous solvents is equivalent to the ratio between activity coefficients seen in Equation (3).

$$\frac{p_{CO2,hyb}}{p_{CO2,aq}} = \frac{\left(\frac{\gamma_{MEAH+} \cdot \gamma_{MEACOO-}}{\gamma_{MEA}^{2}} \right)_{hyb}}{\left(\frac{\gamma_{MEAH+} \cdot \gamma_{MEACOO-}}{\gamma_{MEA}^{2}} \right)_{aq}} \quad (3)$$

The left-leaning shift mentioned before implies that both sides of the expression have positive values greater than one for all of the water-lean solvents studied. It has been previously reported that the activity coefficient of MEA is greater in water-lean solvents than in aqueous ones (Yuan and Rochelle, 2018), which is equivalent to stating that their volatility is increased in the presence of organic diluents. In order to sustain the equality in Equation (3), the increase of the activity coefficients of the electrolytic species must counter the increase in the activity coefficient of MEA. That is to say, the decrease in polarity affects both electrolytes and non-electrolytes, but the former more so than the latter.

Similar considerations may be applied for absorption in solvents containing MDEA, except that MDEA absorbs CO_2 by reacting with water, forming bicarbonate plus protonated MDEA. This can be seen in Equation (4). For 2MPZ, a secondary diamine with two distinct reaction sites, the mechanism is a lot more complex, with several different species being formed as CO_2 is absorbed into the amine (Chen and Rochelle, 2013). Fully describing this mechanism is not within the scope of this work. The ratio between p_{CO2} in hybrid and aqueous solvents should correlate positively to the increase in activity of electrolytic species and negatively with the increase in activity of the amines themselves.

$$CO_2^{(g)} + MDEA^{(l)} + H_2O^{(l)} \xleftrightarrow{K_{eq}} HCO_3^{-(l)} + MDEAH^{+(l)} \quad (4)$$

Since most of the VLE curves observed in this work appear to have the same slope but different intersects, it seems adequate to apply a regression of the form shown in Equation (5), where A is constant for a fixed amine and amine molality but B is different for each hybrid solvent formulation. These B coefficients provide an approximate measurement of the left-leaning shift for each fixed amine and of the effects discussed above. A graphical interpretation of this can be seen in Section 4.1, Figure 2.

$$\ln(p_{CO2}) = A \cdot \alpha + B \quad (5)$$

2.2. Mass transfer rates in water-lean solvents

The flux of CO_2 transported from the bulk of the gas to the bulk of the liquid, N_{CO2}, may be represented by the first line of Equation (6), where K_g is the overall mass transfer coefficient. As its name implies, K_g is dependent on both gas and liquid phase properties. Mass balance requires that this flux is the same through gas and liquid films, respectively lines 2 and 3 from Equation (6). Such treatment conveniently separates gas film contributions from liquid film contributions, so that k_g is the mass transfer coefficient in the gas film and k_g' is the mass transfer coefficient in the liquid film.

$$N_{CO2} = \begin{cases} K_g \cdot \left(p_{CO2}^{gas,b} - p_{CO2}^{liq,b}\right) \\ k_g \cdot \left(p_{CO2}^{gas,b} - p_{CO2}^{\text{int}}\right) \\ k_g^{'} \cdot \left(p_{CO2}^{\text{int}} - p_{CO2}^{liq,b}\right) \end{cases} \quad (6)$$

With Equation (7), k_g' can be recovered from K_g once a good model for k_g is employed. The coefficient obtained in this way is therefore a property of the solvent and can be used for projecting absorber columns.

$$\frac{1}{k_g^{'}} = \frac{1}{K_g} - \frac{1}{k_g} \quad (7)$$

The most interesting phenomenon observed by Yuan and Rochelle (2018) for k_g' in water lean solvents is how steeply it decreases upon CO_2 loading. There is no straightforward way of relating the k_g' measured with other properties of the solvent in order to draw physical insights as those suggested for the VLE shift described previously. An effort in this direction was made by Yuan and Rochelle (2018), who drew from the pseudo-first-order (PFO) assumption to end up with the expression shown in Equation (8).

$$\frac{k_{g,hyb}^{'}}{k_{g,aq}^{'}} = \frac{\left(\frac{D_{CO2}^{0.5} \cdot k_3^{0.5} \cdot \gamma_{MEA}}{\gamma_{CO2}^{0;5}}\right)_{hyb}}{\left(\frac{D_{CO2}^{0.5} \cdot k_3^{0.5} \cdot \gamma_{MEA}}{\gamma_{CO2}^{0;5}}\right)_{aq}} \quad (8)$$

However, this approach has been proven not to work. There are multiple possible reasons for that, all of them suggesting that the PFO simplification is plainly not valid when dealing with water lean solvents. The authors propose that the increased viscosity of water lean solvents upon CO_2 absorption draws them away from PFO to a situation where amine depletion in the interface plays a relevant role in mass transfer rates, and thus the decrease in diffusivity of MEA cannot be neglected (Yuan and Rochelle, 2018). Other explanations could perhaps be found in the investigations of Sada et al. (1985, 1986), who verified an increase in the reaction order of the amine when shifting from an aqueous to a low-aqueous solvent. Though this effect must be taken into consideration in future studies, it is not clear to which extent it would help explaining the phenomena at hand.

There are two ways of comparing the values of k_g's of different solvents: (a) by looking at solvents with a fixed α, and (b) by looking at solvents with a fixed p_{CO2}. The first is scientifically more interesting as it enables a direct analysis of the physical properties of the solvent that affect its mass transfer rate, while the second is more useful for industrial purposes since CO_2 partial pressures at lean and rich ends are usually given parameters of the process at hand. In the biogas upgrading case, biogas rich in CO_2 (up to 40%v/v in most cases) is treated to a stream with circa 98%v/v of methane at atmospheric pressure (TUV, 2012), meaning that the gas stream has to go from p_{CO2} of up 40 kPa at the rich end to 2 kPa at the lean end. The efficiency of CO_2 absorption processes is inversely proportional to the driving forces applied in the absorber, as these driving forces count as work irreversibly lost to the system (Yuan, 2018), and so projecting an efficient absorber for biogas upgrading entails finding a solvent that can be operated at high CO_2 partial pressures. Moreover, since most absorbers are designed with the pinch point close to their rich end, the physical properties (e.g. k_g') of the rich solvent are more relevant for determining the dimensions of the packed column than those of the lean solvent (Jassim and Rochelle, 2006). These two factors are to explain why more emphasis was put on obtaining data at rich rather than at lean loadings during the course of this work.

3. Material and methods

3.1. The solvents tested

The solvents examined in this study were chosen to give a wide view of hybrid solvent properties. For this reason, ethanolamine (MEA) was chosen as the obvious amine candidate representing first generation solvents. It is not only historically the most popular amine for chemical absorption of CO_2 in general (Rochelle et al., 2011), but also one of the mainly used amines for biogas upgrading (TUV, 2012).

For second generation solvents, 2-methylpiperazine (2MPZ) was chosen instead of piperazine (PZ). 2MPZ is an amine of similar structure and properties to PZ which has been suggested to present less precipitation issues than the latter. This is because the methyl group present in 2MPZ confers chirality to the molecule, meaning 2MPZ is usually produced and sold as a racemic mixture of left- and right-handed enantiomers, whose inherent structural differences make bonding and building crystal lattices more complicated in 2MPZ than in PZ (Chen and Rochelle, 2013). Since the precipitation of PZ upon substitution from water to organic diluents is a concern in water lean solvents, 2MPZ is a natural alternative. 2MPZ has the same absorption capacity than PZ, though slightly lower absorption rates (Yuan, 2018).

Finally, MDEA was chosen as the third amine candidate. As MEA is a primary amine and 2MPZ is a secondary amine, including a tertiary amine in this analysis seems fitting. Furthermore, as MDEA and sulfolane blends have been already in use for decades in the industry (Kohl and Nielsen, 1997) and MDEA and MEG blends are being suggested for hydrate inhibition purposes (Akhfash et al., 2017), it is interesting to observe the properties and behavior of these and other similar combinations.

The organic diluents employed in this work are sulfolane (SULF), ethylene glycol (MEG), 1-methylimidazole (1MIMI), dimethyl sulfoxide (DMSO) and N-methyl-2-pyrrolidinone. SULF is a typical physical absorbent used in the oil industry and has been mixed with amines previously in several works (Woertz, 1972; Rivas and Prausnitz, 1979; Leites, 1998). Mixtures of this compound with MDEA are at the heart of the Sulfinol process (Kohl and Nielsen, 1997). MEG is a di-alcohol already in use in the oil industry for its hygroscopic properties. It has also been employed numerous times in the past as diluent for water lean solvents (Semenova and Leites, 1977; Alvarez-Fuster et al., 1981; Sada et al., 1985; Leites, 1998). 1MIMI is an alkyl imidazole, and though no data was found in the literature of it being mixed with amines, blends of amines and imidazoles in general have been recently under consideration (Bara, 2011) and 1MIMI has been proposed on itself as a candidate solvent (Shannon and Bara, 2011). To the extent of this research, no entries were found in the literature for mixtures of DMSO and amines, though this seems like an interesting aprotic diluent similar to SULF. Lastly, NMP is a popular physical solvent employed in the Purisol process for CO_2 absorption. It has also been extensively studied regarding its mixing with amines (Woertz, 1972; Semenova and Leites, 1977; Rivas and Prausnitz, 1979; Leites, 1998; Svensson et al., 2014).

In this work, the molality is defined as mols of amine per kilogram of diluent, wherein by diluent one considers a sum of both water and the organic solvent added to the mixture. This separation between what is the diluent and what is the solute may seem artificial, but it reflects the assumption that the diluent does not take part in the reaction between CO_2 and the 'binder' (i.e. the amine), having simply the task of providing solvation and carbamate stabilization. Furthermore, all solutions are prepared by gravimetry, and their loadings are performed by pumping CO_2 into the solvent and evaluating the change in weight with a scale. As the accuracy of the scale is ± 0.1 g and since about 1.6 kg of solution are prepared for each procedure, loadings are obtained with confidence intervals of ± 10^{-5} mol CO_2/mol N.

Carbamate precipitation was verified in water-lean solvents with 2MPZ prepared with mass ratios (3 organic : 1 water) and molalities as low as 2 m. Therefore, diluent compositions were fixed at (1 organic : 1 water) for all solvents with 2MPZ, and their molalities kept at 2.5 m. Precipitation is rarely an issue for MEA-containing blends, and their diluent compositions could be shifted to (3 organic : 1 water) and molalities increased to 5 m. This seems appropriate as a way of making it plainer to observe the effects of substituting water for non-aqueous diluents. With MDEA, where precipitation is again a possible issue, diluent compositions were kept at (1 organic : 1 water) but molalities were increased to 3.5 m, equivalent of the 30 %w/w typical of most MDEA applications.

More information on the chemicals employed in this work can be found in Table 1. Dipole moments and dielectric permittivities at around 25 °C are displayed for the diluents alone, since they may be interesting for future discussion.

Table 1. Chemicals used in this study and their properties

Name	Structure	Dipole moment (D)	Dielectric permittivity	Role
Carbon dioxide				Gas
Nitrogen				Gas
Ethanolamine (MEA)				Amine
2-methylpiperazine (2MPZ)				Amine
N-methyl diethanolamine (MDEA)				Amine
Water (H2O)		1.85[(1)]	80.4[(5)]	Diluent
Sulfolane (SULF)		4.70[(2)]	43.4[(2)]	Diluent
Ethylene glycol (MEG)		2.75[(3)]	37.0[(5)]	Diluent
1-methylimidazole (1MIMI)		3.80[(1)]	33.4[(6)]	Diluent
Dimethyl sulfoxide (DMSO)		3.96[(1)]	46.7[(7)]	Diluent
N-methyl-2-pyrrolidinone (NMP)		12.26[(4)]	32.7[(4)]	Diluent

[(1)] NIST Chemistry WebBook; [(2)] Tilstam (2012); [(3)] Wu et al. (2017); [(4)] Bezuglaya et al. (2009); [(5)] Maryott and Smith (1951); [(6)] Liu et al. (2017); [(7)] Płowaś et al. (2013)

3.2. Operation of the wetted-wall column (WWC)

The wetted-wall column (WWC) is an apparatus where overall mass transfer coefficients and CO_2 equilibrium partial pressures of a loaded solution can be measured simultaneously. Detailed descriptions of this equipment have been made in previous works (Li et al., 2013; Du et al., 2016). This section gives a brief overview of the method.

Figure (1) shows a schematic depiction of the WWC. At the start of an experiment, an already loaded solvent has to be transferred to the closed loop seen in Figure (1), where it is continuously pumped between a solvent tank and a glass chamber containing one stainless steel pole. After emerging from the tip of the pole, the solvent runs smoothly down its extension, thinly wetting its surface in such a way that the contact area between gas and liquid can be precisely determined as being the same as the surface area of the pole. Solvent temperature is kept constant at a certain set-point by employing a thermal bath coupled with temperature controllers. After the loop is initiated, vapor mixtures of N_2 and CO_2 with predetermined CO_2 content are prepared and fed to the system at controlled rates thanks to two mass flow controllers operating in parallel. This vapor stream goes through a humidifier kept at the same temperature as the system, where it is saturated with water, and then passes through the same thermal bath used for the solvent. This ensures that all points of the loop are at fixed temperature. At the end of the line there is an infrared CO_2 analyzer (Horiba 2000 series) with two modules, one suited for CO_2 concentrations between 0 and 9000 ppm and the other for CO_2 concentrations between 0.1 and 10 %v/v. The whole apparatus can be slightly pressurized, though in general it is preferable to operate it between 238 and 376 kPa (20 and 40 psig). Temperatures can go from room temperature up to as far as 120 °C, but all experiments carried in this work were run at 40 °C.

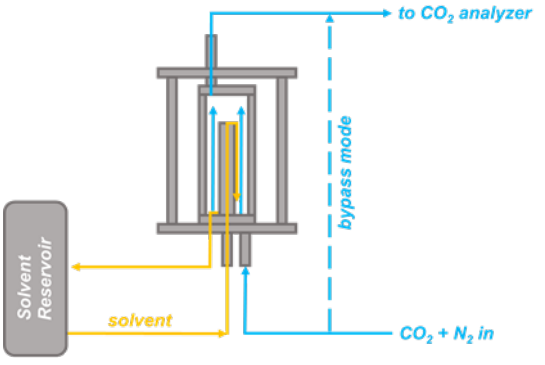

Fig. 1. Schematic drawing of the wetted wall column apparatus

The WWC operates in two different configurations and at two different modes. The two configurations are (a) the bypass configuration, wherein the vapor stream goes directly to the CO_2 analyzer, and (b) the operation configuration, wherein the vapor stream is made to first contact the solvent in the wetted wall. In practical terms, CO_2 concentrations measured in the bypass configuration are the inlet flow of CO_2, whereas those measured in the operation configuration refer to outlet flow. With both these values, flux of CO_2 into the solvent can be estimated by Equation (9).

$$N_{CO2} = \left(\frac{p_{CO2}^{in} - p_{CO2}^{out}}{p} \right) \cdot \frac{Q_{gas}}{S} \tag{9}$$

The two modes are desorption mode and absorption mode. If the inlet gas stream has lower CO_2 partial pressure than the equilibrium partial pressure of the loaded solvent, then the outlet gas stream will have higher CO_2 content. This is the desorption mode. Conversely, in the absorption mode, the inlet stream has higher CO_2 partial pressure than that in equilibrium with the solvent, causing the outlet stream to have lower CO_2 content. In a confined span around p_{CO2} at the bulk of the solvent, the relationship between p_{CO2}^{in} and p_{CO2}^{out} is practically linear, and p_{CO2} may be estimated by regressing a line and setting $p_{CO2}^{in} = p_{CO2}^{out} = p_{CO2}$. Then, once p_{CO2} is estimated, the driving force for each flux obtained in Equation (9) can be calculated by Equation (10).

$$\Delta u = \frac{\left(p_{CO2}^{in} - p_{CO2}\right) - \left(p_{CO2}^{out} - p_{CO2}\right)}{\ln\left(\frac{p_{CO2}^{in} - p_{CO2}}{p_{CO2}^{out} - p_{CO2}} \right)} \tag{10}$$

The driving force shown in Equation (10) is nothing but a logarithmic average of the difference in CO_2 partial pressures between gas and liquid bulks throughout the system. Comparison with the first line of Equation (6) shows that the quotient of Equations (9) and (10) should result in K_g, though a more robust methodology is to take several points for different values of N_{CO2} and Δu and find K_g by linear regression. In this work, 6 – 7 points divided between desorption and absorption mode were taken for each loaded solution and dually regressed to obtain p_{CO2} and K_g with a good margin of confidence. With the estimated K_g and a model for k_g, k_g' can be readily recovered.

There are a few factors constraining the span of data gathered with the WWC. The accuracy of the mass flow controllers and of the CO_2 analyzer coupled with the operational window 1.4 – 2.8 bar for pressure in the glass chamber implies that fluxes of CO_2 are too unstable in the lower end and simply un-analyzable in the higher end. The first issue is solved by employing a pre-prepared mixture of N_2 and CO_2 with 5000 ppm CO_2 bought from Praxair, but the second issue remains for the time being. A third issue, related to k_g, will be mentioned shortly.

Though no reproducibility analyses were performed in this work, the performance of this same apparatus has been asserted by Yuan (2018) to give consistent and correct results. The sensitivity of the CO_2 analyzer is of ± 1 ppm CO_2 in the low partial pressure mode and ± 100 ppm CO_2 in high partial pressure mode. A detailed procedure to obtain the confidence intervals for the p_{CO2} measurements is given in the Appendix B. Since K_g is reliant on p_{CO2}, its uncertainty is proportionally higher. Calculation of these uncertainties is also explained in Appendix B.

4. Results and discussion

4.1. Results and discussion for the proposed water lean solvents

Figures 2(a), 2(b) and 2(c) show respectively sets of VLE points obtained for blends of MEA, 2MPZ and MDEA with various organic diluents. They are a good example of the approach suggested in previous sections. The shift in chemical equilibrium could be conveniently estimated by regressing a set of parallel lines from the VLE data obtained in the WWC – that is, by performing a regression with all data points simultaneously with the condition that the lines obtained have equal slope. The vertical distances between parallel lines in all three images is a graphical indication of the values of B, the coefficient previously mentioned in Eq. (5).

At times, this regression seems reasonably to represent the data, as is the case with the MDEA plots in Figure 2(b). One can see that this does not necessarily happen in Figure 2(a), where data for water-lean solvents with SULF and DMSO plus MEA are particularly badly fitted. However, the suggested interpretation of these fittings is that they represent an average or at least a trend. Therefore, in Figure 2(a), the equilibrium shift with NMP appears to be in average stronger than that with 1MIMI, which is stronger than that with MEG and so on. This trend is numerically conveyed through the regressed parameters. Furthermore, fixing the slope of the curves for each family of solvents outlines the capacity for CO_2 absorption of the amines themselves. Capacity of the 2.5 m 2MPZ blends was observed to be about 15% higher than that of 5 m MEA blends and 80% higher than that of 3.5 m MDEA blends, as defined by the ratios between the slopes obtained.

With this approach in terms of linearization and averaging, one may lose sight of some interesting information, such as the fact that MEA + 1MIMI apparently overtakes MEA + NMP in terms of performance at higher loadings, as seen in Figure 2(a). However, this enables the treatment shown later on in this Section and in Section 4.3.

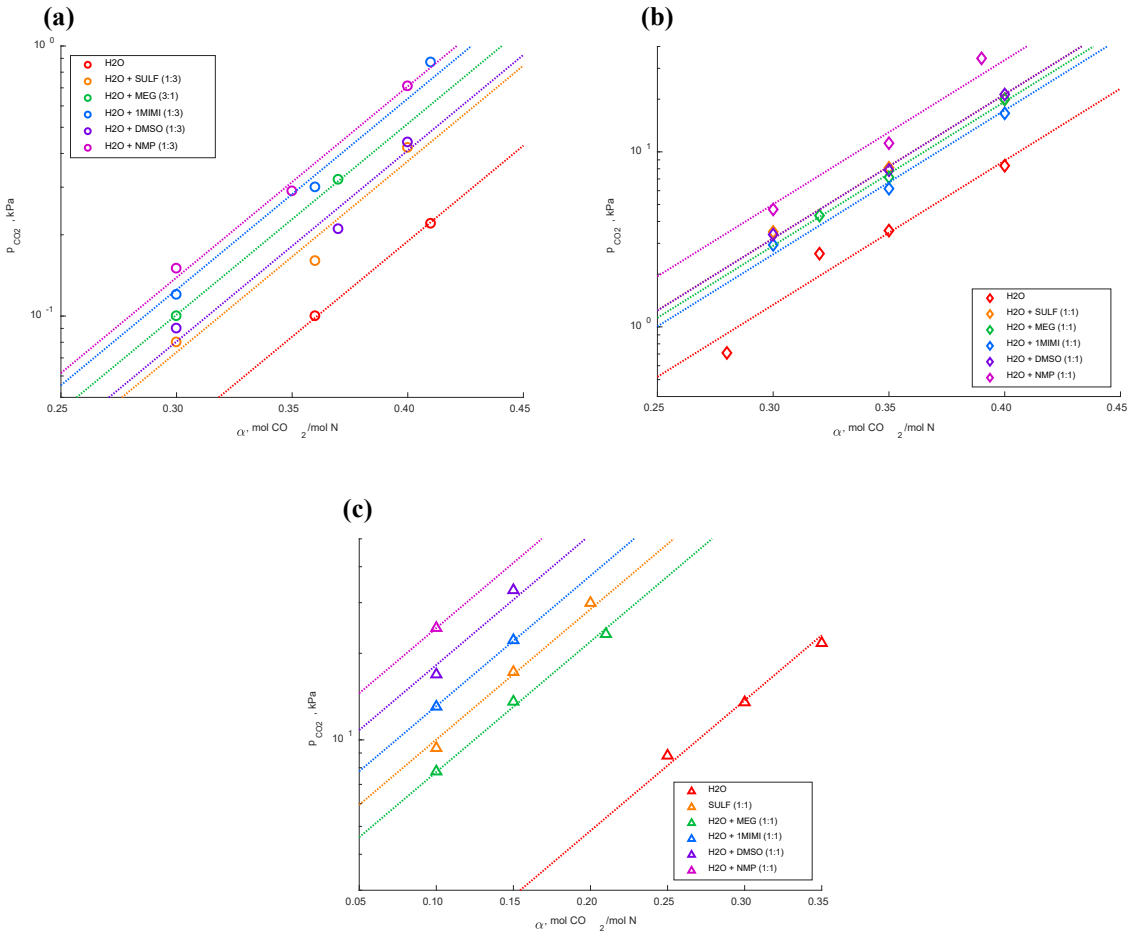

Fig. 2. (a) VLE curves for 5 m MEA solvents regressed with data from the WWC at 40 °C; (b) VLE curves for 2.5 m 2MPZ solvents regressed with data from the WWC at 40 °C; (c) VLE curves for 3.5 m MDEA solvents regressed with data from the WWC at 40 °C

Figure 3 quantifies the left-leaning shift for each solvent tested in this study. Figure 3(a) presents it simply as it is, while Figure 3(b) plots the values against the dielectric permittivity of each diluent estimated by using the properties shown in Table 1 plus a mixing relation suggested elsewhere (Reynolds and Hough, 1957) divided by that of pure water.

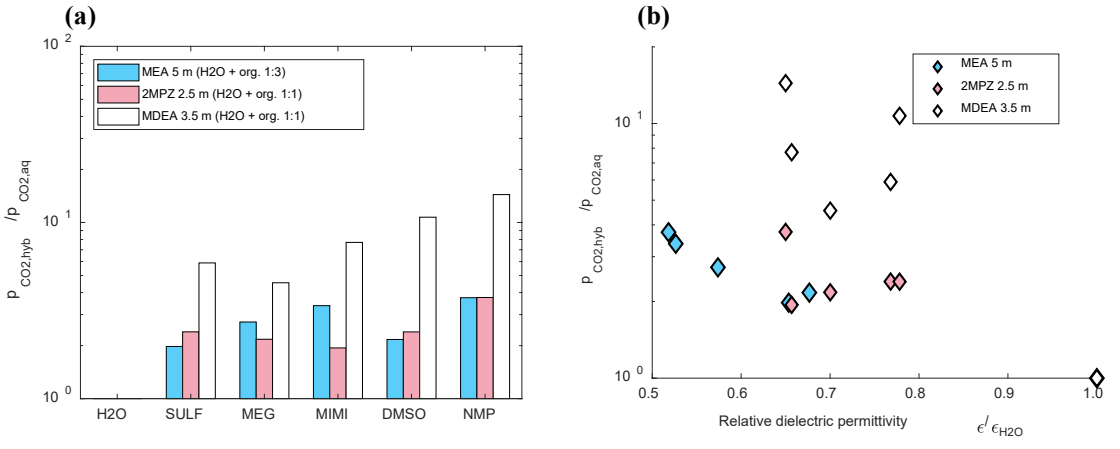

Fig. 3. (a) Chemical equilibrium shift observed in water lean solvents at 40 °C in the WWC; (b) an outline of the chemical equilibrium shift as a function of changing the dielectric permittivity of the medium

As seen in Figure 3(a), addition of organic diluents to the mixtures incites a left-leaning shift in all of the systems studied. The magnitude of this shift is substantially greater in water lean solvents containing 3.5 m MDEA than in water lean solvents with 5 m MEA, even though the amount of organic diluents added to these solutions is proportionally smaller. Looking back at Equation (3), this seems to suggest that either:

- The de-stabilization of the electrolytes in MDEA solutions (i.e. the increase of their activity coefficients) is greater with the decrease in polarity of the medium; or that
- The de-stabilization of the reagents in MDEA solutions (i.e. the increase of their activity coefficients) is smaller with the decrease in polarity of the medium.

Both effects would explain the behavior observed in the course of these experiments. It seems unlikely, however, that the activities of species $MDEAH^+$ and HCO_3^- would be more dependent on the polarity of the medium than the activities of species $MEAH^+$ and $MEACOO^-$. Therefore, it is tempting to describe this phenomenon through the stability of the reactants themselves. It is known that MDEA is a less polar molecule than MEA, and it is expected that a decrease in polarity of the solvent will increase the activity of MEA more than it does to MDEA. Furthermore, since the stoichiometry of reaction between CO_2 and MEA is 1:2 whereas that between CO_2 and MDEA is 1:1, the VLE shift in MEA solutions is more sensitive to the activity of the amine than that in MDEA solutions. The cumulative effect of less de-stabilization of the amine upon addition of an organic diluent plus less compensation through this increase in activity may explain the huge shift observed in Figure 3.

Figure 3(a) also shows that relative magnitudes of the left-leaning shift are less clear when dealing with 2MPZ solvents, perhaps because the lower content of organic diluent in those mixtures confounds the results. For the cases with SULF, DMSO and NMP, it is clear that the increase in p_{CO2} upon reduction in polarity of the medium is stronger for 2MPZ solvents than for MEA. Once again, this might imply that the higher polarity of MEA with regards to 2MPZ makes this amine more susceptible to increases in activity when an organic diluent is added. However, for the organic diluents MEG and 1MIMI, no conclusions can be made with this respect.

Others have suggested (Sada et al., 1985, 1986; Leites, 1998) that higher dielectric permittivities imply more stabilization towards the intermediaries and products of the reactions between amines and CO_2. Hamborg et al. (2010, 2011) particularly implied that the base strength of the amine is dependent on this parameter. Figure 3(b) shows that, in the case of MEA, there is a good trend of exponential decrease between the chemical equilibrium shift and the dielectric permittivity of the medium. However, this pattern breaks down for solvents with 2MPZ and MDEA, particularly for the latter.

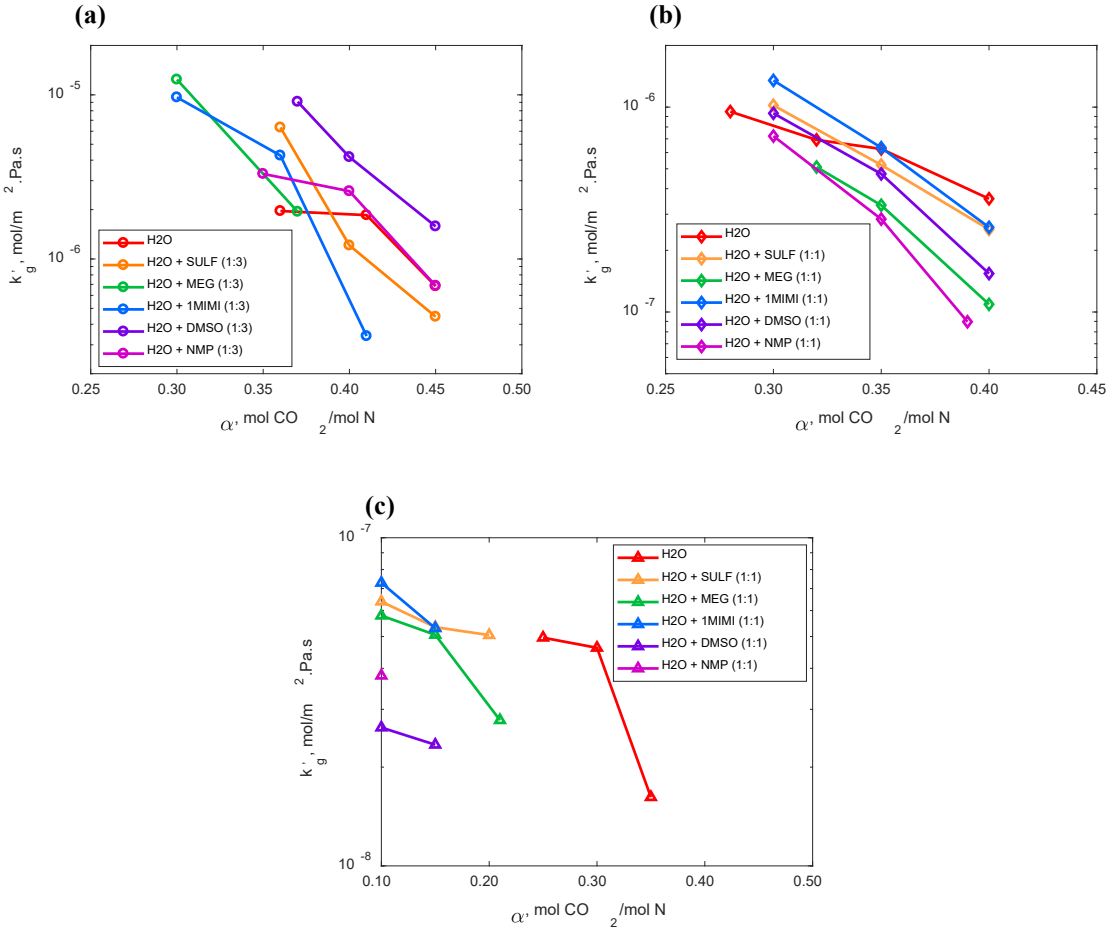

Fig. 4. (a) Mass transfer coefficients in 5 m MEA plus various diluents at 40 °C; (b) mass transfer coefficients in 2.5 m 2MPZ plus various diluents at 40 °C; (c) mass transfer coefficients in 3.5 m MDEA plus various diluents at 40 °C

Figures 4 and 5 show the liquid-film mass transfer coefficients k_g' obtained for the water lean solvents in this study both in terms of loading α (Figure 4) as in terms of CO_2 partial pressure p_{CO2} (Figure 5).

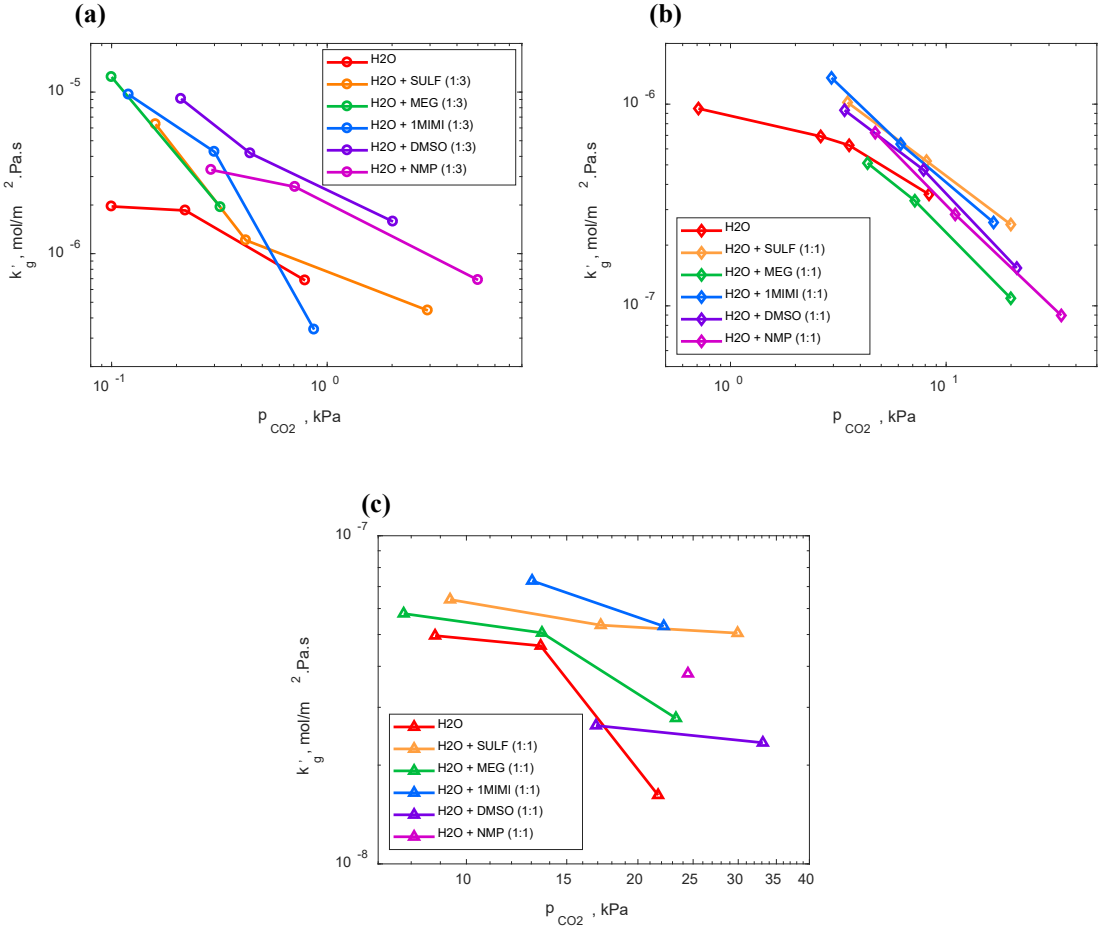

Fig. 5. (a) Mass transfer coefficients in 5 m MEA plus various diluents at 40 °C; (b) mass transfer coefficients in 2.5 m 2MPZ plus various diluents at 40 °C; (c) mass transfer coefficients in 3.5 m MDEA plus various diluents at 40 °C

Looking back at Equation (8), if the PFO assumption is assumed valid, one could assume that the addition of organic diluents would, for a fixed loading α:

- Decrease the diffusivity of CO_2, D_{CO2}, in result of the increase in viscosity of the medium;
- Decrease the reaction rate k_3 of the direct reaction, as Sada et al. (1985, 1986) proposed that such a rate is inversely dependent on the logarithm of ε in result of less stabilization of intermediaries and products through salvation effects;
- Increase the activity coefficient of the amine, as discussed previously; and
- Decrease the activity coefficient of CO_2 due to the higher physical solubility of the acid gas in water lean solvents.

Whatever the net result of these four factors is, the findings of the experiments carried in this research show that, for 5 m MEA at lean loadings, addition of all five proposed organic diluents increase mass transfer rates. Figure 5(a) shows that at higher loadings, however, this advantage might diminish or disappear. For example, addition of 1MIMI and MEG stops making up for competitive solvents at higher loadings, as evidenced by how steeply k_g' decreases with p_{CO2} in Figure 5(a). On the other hand, both DMSO and NMP seem to consistently increase k_g'. This agrees to what was observed by Yuan and Rochelle (2018) for the addition of NMP to MEA 7 m. Once the left-

leaning shift is considered and k_g' is accounted for a fixed p_{CO2} instead of α, addition of all organic diluents seem to increase the mass transfer rate of CO_2 in 5 m MEA in the order DMSO > NMP > 1MIMI > MEG. Essentially, the shift in equilibrium caused by the inclusion of an organic diluent means that more free amine is present to react at the interface for a given CO_2 partial pressure.

A similar behavior is observed for solvents with 2.5 m 2MPZ. In terms of loading, as seen in Figure 4(b), addition of almost all organic diluents (the exception being MEG) seems to increase the mass transfer rates in the lean end. In the rich end, any advantage disappears and aqueous 2MPZ emerges as having the higher k_g' for CO_2 absorption. In terms of p_{CO2}, with the equilibrium shift in view, almost all water lean solvents appear to be competitive with regards to their aqueous counterpart in the order SULF > 1MIMI > DMSO > NMP. This is apparent in Figure 5(b). MEG consistently does not increase the k_g' of 2.5 m 2MPZ.

Finally, for MDEA, the shift in the reaction equilibrium is so strong that it is virtually impossible to compare the solvents at a same loading with the data obtained from the experiments, Figure 4(c). In terms of p_{CO2}, as seen in Figure 5(c), all of them seem to be competitive in the order 1MIMI > SULF > NMP > DMSO > MEG.

In general, it seems that the conjoint effects of equilibrium shift and mass transfer rate increase can raise the attractiveness of certain blends of water lean solvents. However, these effects seem to be dependent on both the characteristics of the amine and those of the diluent, with no clear ranking showing what the best diluent could be for a generic case. NMP is confirmed as being a very promising physical absorbent to be mixed with MEA, but not so with 2MPZ or MDEA. On the other hand, 1MIMI works pretty well with 2MPZ and MDEA-based solvents, but not so much with MEA, though it can promote the absorption of CO_2 even at higher loadings where that of aqueous MEA begins dropping steeply. Both DMSO and SULF have shown consistently good results with all three amines, though being surpassed in each scenario by one or more of the other diluents. In all cases studied, MEG does not seem to improve significatively the mass transfer properties of the amine blends.

All of these considerations neglect the impact that the viscosities of water lean solvents have in the overall efficiency of the process. Yuan (2018) shows a comprehensive analysis of the whole CO_2 capture plant and demonstrates that the capital costs of dealing with high viscosities in the heat exchangers may easily surpass whatever is gained by operating with a smaller packed column. Other issues pertaining water lean solvents, such as the higher volatilities of amines and diluent themselves, may render operation with such mixtures more of a burden than these results suggest. Furthermore, what can be noticed in Figure 4 is that all advantages with regards to k_g' in water lean solvents decrease steeply at the rich end of the loading spectrum. As discussed above, this is usually the end that is more relevant on determining the dimensions of the packed column.

For biogas upgrading purposes, aqueous 5 m MEA does not seem like a promising solvent for CO_2 capture. This is evident by comparison of Figures 5(a) and 5(b), where the k_g' of aqueous MEA takes a dive before reaching partial pressures typical of untreated raw biogas. In view of this, mixing with NMP or DMSO could come as beneficial for absorbing at higher partial pressures with the high mass transfer coefficients typical of MEA-based solvents. Unfortunately, no data was gathered at high pressures for these blends, and one cannot assume that their k_g' will not drop dramatically once amine depletion becomes more relevant as it did to aqueous MEA. As an example: Table 2 shows that 5 m MEA + NMP blends have a similar kg' to aqueous 2.5 m 2MPZ, but one should not forget that these are values referent to different loadings. It is quite likely that the k_g' of the MEA-based solvent will drop faster than that of 2MPZ, given that the latter is operating closer to amine depletion stage.

Both 2MPZ and MDEA-based solvents seem to keep their mass transfer coefficients reliably at somewhat stable values under high CO_2 partial pressures, though 2.5 m 2MPZ absorbs CO_2 5 to 10 times faster. Table 2 shows some values for k_g' at 10 and 20 kPa for the most competitive MEA, 2MPZ and MDEA solvents discussed in this research.

Table 2. Interpolated values for the liquid-film mass transfer coefficients for a variety of solvents studied

Solvent	k_g' at 10 kPa (mol/Pa.m^2.s)	k_g' at 20 kPa (mol/Pa.m^2.s)
5 m MEA in H2O + NMP (1:3)	$3.3.10^{-7}$*	--
5 m MEA in H2O + DMSO (1:3)	$4.6.10^{-7}$*	--
2.5 m 2MPZ in H2O	$3.3.10^{-7}$	$1.7.10^{-7}$
2.5 m 2MPZ in H2O + SULF (1:1)	$4.4.10^{-7}$	$2.5.10^{-7}$
2.5 m 2MPZ in H2O + 1MIMI (1:1)	$4.2.10^{-7}$	$2.1.10^{-7}$
3.5 m MDEA in H2O	$4.9.10^{-8}$	$2.1.10^{-8}$
3.5 m MDEA in H2O + SULF (1:1)	$6.3.10^{-8}$	$5.2.10^{-8}$

* These values were extended from the results displayed in Figure 3(a) and may grossly misrepresent reality in case a sudden drop in k_g' is to be seen between the last data point obtained experimentally and p_{CO2} = 10 kPa

The results interpolated in Table 2 show that, even if one is optimistic regarding the behavior of the mass transfer rates in water lean solvents containing 5 m MEA and no sudden drop in k_g' is to be seen, aqueous 2.5 m 2MPZ still displays comparatively fast absorption rates. When blended with diluents such as SULF or 1MIMI, these rates are even higher and stay higher at p_{CO2} = 20 kPa, though their advantage is reduced at higher partial pressures as seen in Figure 4(b). 2MPZ-based solvents also absorb CO_2 substantially faster than MDEA-based solvents. The results of this investigation seem to suggest that second generation solvents such as 2MPZ are more indicated for amine scrubbing in the biogas context than first generation ones. This comes due to faster absorption rates and to 2MPZ having increased capacity for CO_2 absorption even when in equilibrium with CO_2 at higher partial pressures, meaning the absorption-desorption process can be carried more reversibly than what is usually possible with MEA.

4.2. Further investigations on the effects of diluents in water lean solvents

Data obtained from Dugas (2009) and from Yuan (2018), as well as previously unreleased data obtained from the research performed at the NTNU, has been compiled to better contemplate the equilibrium shift in water lean solvents. The results of this analysis give more of an overview than a comprehensive interpretation of the observed phenomena. Therefore, this section is intended in pointing out areas where more understanding is needed.

In previous sections, the proportions of water, organic diluents and amines have been kept constant for a fixed amine family. When amine concentrations and organic to water proportions are allowed to vary, the picture becomes even more blurred. For instance, in Figure 6(a) one can see the shift to the left in low- and now-aqueous solvents with THFA (tetrahydrofurfuryl alcohol) plus MEA with different molalities. From a distance, these curves seem to form a simple pattern: the more organic diluent is added, the stronger is the equilibrium shift. This is to be expected as, essentially, a progressive decrease in the dielectric permittivity is being performed for each of these series. However, closer inspection shows that the strength of this shift also grows in the order 4.1 m > 7.0 m > 1.8 m. There are currently no conclusive explanations for this phenomenon.

Figure 6(b) shows the VLE data for solvents with PZ (piperazine) 5 m at 40 °C, all obtained in the wetted wall column. Aqueous PZ data was obtained by Dugas (2009), and subsequent hybrid formulations were tested by Yuan (2018). For PZ, there is hardly a parallelism in the VLE curves in aqueous and water lean solvents. One can even observe a point for the VLE curve of aqueous sulfolane (1:1) plus PZ in which the CO_2 partial pressure is lower than in aqueous PZ at the same loading. Assuming this data is correct, this is an interesting case of "reverse cross-over pressure", an event previously described in the literature (Song et al., 1997; Leites, 1998) in which for low loadings the CO_2 solubility in water lean solvents is higher than in aqueous solvents. Evidently, the set of reactions involving CO_2 and PZ is more complex than the one involving CO_2 and MEA. The curves in Figure 6(b) make it clear that the treatment of VLE data by means of a simple shift to the left in water lean solvents is highly specific to very simple scenarios. For several other applications, deeper understanding is still lacking.

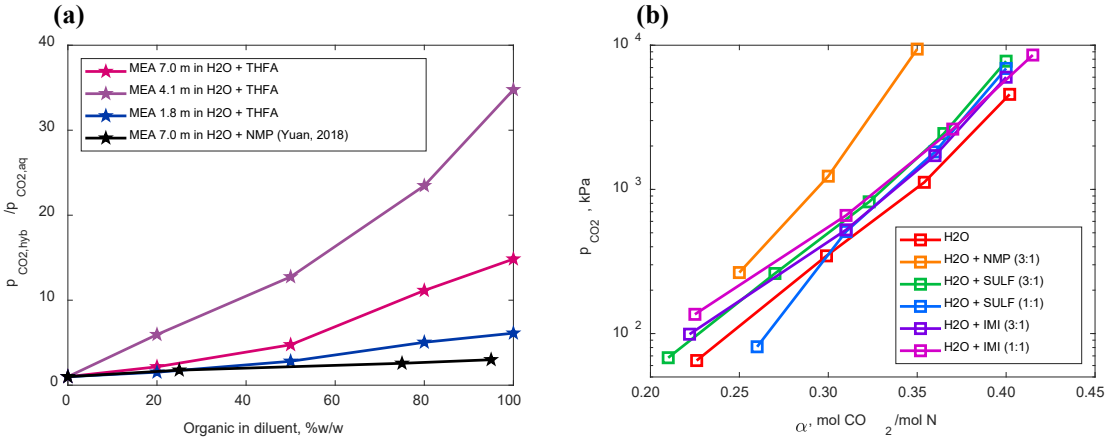

Fig. 6. (a) The ratio between CO_2 partial pressure p_{CO2} in hybrid and aqueous solvents at a fixed loading α for various amines, all data at 40 °C; (b) Equilibrium curves for water lean solvents with PZ 5 m at 40 °C obtained by Dugas (2009) and Yuan (2018), IMI = imidazole

The behavior of the VLE curves with shifting dielectric permittivities observed in Figure 3(b) is quite baffling. For 5 m MEA, the observed trend is congruent with expectations set out by multiple authors (Sada et al. 1985, 1986; Leites, 1998; Hamborg et al., 2010, 2011) in which a decrease in dielectric permittivity causes a strong equilibrium shift. However, for 2.5 m 2MPZ and 3.5 m MDEA, there is no clear pattern. Rather than solving this issue, this work will merely suggest a possible approach.

In their original work (Sada et al., 1985), Sada et al. implied a connection between kinetic constants and the Hildebrandt solubility parameter (δ) of the diluent, which on its part is linearly related to the dielectric permittivity of the medium. Lately, an effort has been made in dividing δ in three components: a component related to the London dispersion forces of the solvent (δ_d), a component related to its permanent dipole forces (δ_p) and a component related to its hydrogen bond forces (δ_h). These are the Hansen solubility parameters (Hansen, 2007). Values of these parameters are conveniently available for all organic diluents tested in this work, as well as mixing rules to calculate their values in low-aqueous mixtures (Hansen, 2007). If one is to assume that the original observation by Sada et al. (1985) can be extended from the Hildebrandt parameter to the Hansen parameters, or rather to a linear combination of the three Hansen parameters, and that the coefficients of this linear combination are a function of the amine species in solution, then a fitting can be made with the form outlined in Equation (11).

$$\ln\left(\frac{p_{CO2,hyb}}{p_{CO2,aq}}\right) = C_1 \cdot \delta_d + C_2 \cdot \delta_p + C_3 \cdot \delta_h \tag{11}$$

Once the parameter fitting was done for 5 m MEA, 2.5 m 2MPZ and 3.5 m MDEA, the coefficients obtained were as shown in Table 3. These coefficients have also been normalized so that their relative strengths can be better assessed. Table 3 clearly shows that the effects of hydrogen bonding interactions are a lot less significant than that of London forces and dipole-dipole interactions. A visualization of this approach can be seen on Figure 7, which only demonstrates the quality of the fitting done with the coefficients shown in Table 3.

Table 3. Coefficients found for the Hansen solubility parameter correlation

Amine	C_1	C_2	C_3	$\|C_1\|.100\%$	$\|C_2\|.100\%$	$\|C_3\|.100\%$
5 m MEA	0.1897	-0.1347	-0.0118	66.3%	33.4%	0.3%
2.5 m 2MPZ	0.2463	-0.1531	-0.0358	71.0%	27.5%	1.5%
3.5 m MDEA	0.5550	-0.3174	-0.1113	73.1%	23.9%	3.0%

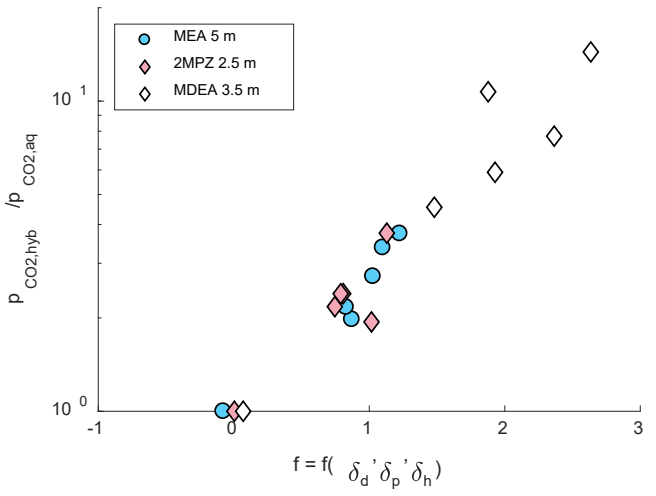

Fig. 7. Equilibrium shift as a linear function of the Hansen solubility parameters for multiple amines at 40 °C. For 5 m MEA: **$f=0.1897*\delta_d-0.1347*\delta_p-0.0118*\delta_h$**. For 2.5 m 2MPZ: **$f=0.2463*\delta_d-0.1531*\delta_p-0.03458*\delta_h$**. For 3.5 m MDEA: **$f=0.5550*\delta_d-0.3174*\delta_p-0.1113*\delta_h$**. In other words, the coefficients for the linear functions plotted are the ones found in Table 3.

As seen through the coefficients in Table 3, moving from aqueous to water lean solvents can be roughly said to have two main consequences: a change in the dispersion forces and a change in the dipole forces. For all amines, the equilibrium shift is stronger if the dispersion forces are increased and the dipole forces are reduced. This seems reasonable. The London dispersion forces can be related to induced dipole interactions typical of non-polar molecules, and both intermediaries and products of amine reactions with CO_2 are strongly polar, and thus de-stabilized the bigger the δ_d. They are, however, stabilized by strong polar interaction, and so the bigger the δ_p the weaker is the equilibrium shift.

The differences observed between MEA, 2MPZ and MDEA are related to how effective these stabilization/de-stabilization mechanisms are for each different amine. Therefore, while in the past the dielectric permittivity has been the focus on interpreting equilibrium shift data in water lean solvents, it is suggested that other forms of intermolecular interactions (namely London forces and, to a lesser extent, hydrogen bonding forces) should be taken into consideration in future works.

5. Conclusion

Addition of an organic diluent to a solvent has several effects. Two of them were particularly studied in this research, namely a chemical shift (i.e. shift in activities of both electrolytic species and amines) and the promotion of liquid-film mass transfer coefficients. While the chemical shift causes the CO_2 partial pressure in equilibrium above a certain loading to be higher in water lean solvents than in their aqueous counterparts, promotion of mass transfer rates induces faster rates for the same CO_2 partial pressure (though not necessarily for the same loading). The net effect of these phenomena is a solvent that can be best suited for capturing CO_2 under high partial pressures, which is precisely the case for biogas upgrading.

Some parameters were proposed to correlate these effects with physical properties of the organic diluents. Regarding the chemical shift, the dielectric permittivity ε seems to have a direct influence over the activities of reagents and products: the lower the ε, the higher the shift towards unreacted amine. This observation can be correlated to the solvation properties of the diluent and their resulting de-stabilization on intermediaries and products. Another possible approach is relating chemical equilibrium to the Hansen solubility parameters of the diluents. Furthermore, the chemical shift is found to be stronger in MEA-based solvents than in MDEA-based

solvents, perhaps due to the stoichiometry of the reaction or perhaps due to the higher polarity of MEA when compared to MDEA.

No general rule was observed regarding how different diluents affect different amine solvents in matters of mass transfer rates. NMP has a positive effect on the mass transfer coefficient of MEA-based solvents, while 1MIMI seems more suited to 2MPZ and MDEA-based solvents. DMSO and SULF showed good results for all amines, though in each case they were surpassed by some of their alternatives. MEG does not show many interesting properties at all, at least concerning promoting mass transfer rates in water lean solvents.

Second generation solvents with 2MPZ were found to be best suited for capturing CO_2 under higher CO_2 partial pressures than first generation solvents either with MEA or MDEA, regardless of the presence of organic diluents in the mixture. Water lean solvents with 2MPZ may have higher mass transfer coefficients than aqueous 2MPZ, but their advantage decreases quickly under high CO_2 partial pressures.

Other properties essential for engineering better solvents in more efficient processes, among which one should mention viscosities and volatilities, were not emphasized in the current research. There are reasons to suspect that they may pose a bigger issue in hybrid formulations than in regular aqueous solvents. Therefore, they should be decisively approached in any future work regarding amino-organic mixtures for CO_2 capture.

Acknowledgements

This research was funded by the Faculty of Natural Sciences of the Norwegian University of Science and Technology (NTNU), the University of Texas at Austin and the Research Council of Norway (RCN) under project number 289346.

Appendix A. Data obtained in the WWC

A.1. Data for 5 m MEA solvents

Table 4. Data obtained for MEA-based water lean solvents in the WWC at 40 °C

α (mol CO_2/mol N)	p_{CO2} (kPa)	K_g (mol/m^2.s.Pa)	k_g (mol/m^2.s.Pa)	k_g' (mol/m^2.s.Pa)
5 m MEA in water				
0.36	0.102 ± 0.004	(1.1 ± 0.1).10^{-6}	(2.9 ± 0.3).10^{-6}	(1.9 ± 0.3).10^{-6}
0.41	0.22 ± 0.02	(1.1 ± 0.1).10^{-6}	(2.9 ± 0.3).10^{-6}	(1.8 ± 0.3).10^{-6}
0.45	0.79 ± 0.04	(5.5 ± 0.5).10^{-7}	(2.9 ± 0.3).10^{-6}	(6.8 ± 0.9).10^{-7}
5 m MEA in water + SULF (1:3)				
0.30	0.083 ± 0.009			
0.36	0.16 ± 0.03	(1.8 ± 0.2).10^{-6}	(2.5 ± 0.2).10^{-6}	(6 ± 3).10^{-6}
0.40	0.42 ± 0.05	(7.7 ± 0.8).10^{-7}	(2.1 ± 0.2).10^{-6}	(1.2 ± 0.2).10^{-6}
0.45	2.9 ± 0.2	(3.7 ± 0.4).10^{-7}	(2.1 ± 0.2).10^{-6}	(4.4 ± 0.5).10^{-7}
5 m MEA in water + MEG (1:3)				
0.30	0.105 ± 0.009			
0.37	0.32 ± 0.04	(7.8 ± 0.8).10^{-7}	(1.3 ± 0.1).10^{-6}	(1.9 ± 0.6).10^{-6}
5 m MEA in water + 1MIMI (1:3)				
0.30	0.122 ± 0.007	(2.2 ± 0.2).10^{-6}	(2.9 ± 0.3).10^{-6}	(1.0 ± 0.5).10^{-5}
0.36	0.30 ± 0.01	(1.7 ± 0.2).10^{-6}	(2.9 ± 0.3).10^{-6}	(4 ± 1).10^{-6}
0.41	0.87 ± 0.05	(2.3 ± 0.2).10^{-7}	(7.3 ± 0.7).10^{-7}	(3.4 ± 0.5).10^{-7}
5 m MEA in water + DMSO (1:3)				
0.30	0.08 ± 0.01			
0.37	0.20 ± 0.02	(2.0 ± 0.2).10^{-6}	(2.5 ± 0.2).10^{-6}	(9 ± 5).10^{-6}

0.40	0.442 ± 0.006	$(1.6 \pm 0.2).10^{-6}$	$(2.5 \pm 0.2).10^{-6}$	$(4 \pm 1).10^{-6}$
0.45	2.0 ± 0.3	$(9.7 \pm 0.1).10^{-7}$	$(2.5 \pm 0.2).10^{-6}$	$(1.6 \pm 0.3).10^{-6}$
5 m MEA in water + NMP (1:3)				
0.30	0.14 ± 0.01			
0.35	0.29 ± 0.03	$(1.4 \pm 0.1).10^{-6}$	$(2.5 \pm 0.2).10^{-6}$	$(3.3 \pm 0.9).10^{-6}$
0.40	0.71 ± 0.03	$(1.3 \pm 0.1).10^{-6}$	$(2.5 \pm 0.2).10^{-6}$	$(2.6 \pm 0.6).10^{-6}$
0.45	5.0 ± 0.4	$(5.4 \pm 0.5).10^{-7}$	$(2.5 \pm 0.2).10^{-6}$	$(6.9 \pm 0.9).10^{-7}$

A.2. Data for 2.5 m 2MPZ solvents

Table 5. Data obtained for 2MPZ-based water lean solvents in the WWC at 40 °C

α (mol CO_2/mol N)	p_{CO2} (kPa)	K_g (mol/m^2.s.Pa)	k_g (mol/m^2.s.Pa)	k_g' (mol/m^2.s.Pa)
2.5 m 2MPZ in water				
0.20	0.29 ± 0.03	$(1.3 \pm 0.1).10^{-6}$	$(2.9 \pm 0.3).10^{-6}$	$(2.5 \pm 0.5).10^{-6}$
0.28	0.70 ± 0.03	$(6.3 \pm 0.6).10^{-7}$	$(1.9 \pm 0.2).10^{-6}$	$(9 \pm 2).10^{-7}$
0.32	2.62 ± 0.05	$(5.0 \pm 0.5).10^{-7}$	$(1.9 \pm 0.2).10^{-6}$	$(6 \pm 1).10^{-7}$
0.35	3.6 ± 0.3	$(5.1 \pm 0.5).10^{-7}$	$(2.9 \pm 0.3).10^{-6}$	$(6.2 \pm 0.8).10^{-7}$
0.40	8.3 ± 0.8	$(3.0 \pm 0.3).10^{-7}$	$(1.9 \pm 0.2).10^{-6}$	$(3.6 \pm 0.4).10^{-7}$
2.5 m 2MPZ in water + SULF (1:1)				
0.30	3.5 ± 0.2	$(7.5 \pm 0.7).10^{-7}$	$(2.9 \pm 0.3).10^{-6}$	$(1.0 \pm 0.1).10^{-6}$
0.35	8.1 ± 0.6	$(4.1 \pm 0.4).10^{-7}$	$(1.9 \pm 0.2).10^{-6}$	$(5.2 \pm 0.7).10^{-7}$
0.40	20 ± 2	$(1.9 \pm 0.2).10^{-7}$	$(7.3 \pm 0.7).10^{-7}$	$(2.5 \pm 0.3).10^{-7}$
2.5 m 2MPZ in water + MEG (1:1)				
0.32	4.3 ± 0.3	$(4.3 \pm 0.4).10^{-7}$	$(2.9 \pm 0.3).10^{-6}$	$(5.1 \pm 0.6).10^{-7}$
0.35	7.2 ± 0.4	$(2.8 \pm 0.3).10^{-7}$	$(1.9 \pm 0.2).10^{-6}$	$(3.3 \pm 0.4).10^{-7}$
0.40	20 ± 2	$(9.5 \pm 0.9).10^{-8}$	$(7.3 \pm 0.7).10^{-7}$	$(1.1 \pm 0.1).10^{-7}$
2.5 m 2MPZ in water + 1MIMI (1:1)				
0.30	2.9 ± 0.2	$(9.2 \pm 0.9).10^{-7}$	$(2.9 \pm 0.3).10^{-6}$	$(1.3 \pm 0.2).10^{-6}$
0.35	6.2 ± 0.2	$(4.7 \pm 0.5).10^{-7}$	$(1.9 \pm 0.2).10^{-6}$	$(6.3 \pm 0.9).10^{-7}$
0.40	17 ± 1	$(2.1 \pm 0.2).10^{-7}$	$(1.0 \pm 0.1).10^{-6}$	$(2.6 \pm 0.3).10^{-7}$
2.5 m 2MPZ in water + DMSO (1:1)				
0.30	3.4 ± 0.2	$(7.0 \pm 0.7).10^{-7}$	$(2.9 \pm 0.3).10^{-6}$	$(9 \pm 1).10^{-7}$
0.35	7.0 ± 0.7	$(3.8 \pm 0.4).10^{-7}$	$(1.9 \pm 0.2).10^{-6}$	$(4.7 \pm 0.6).10^{-7}$
0.40	21 ± 2	$(1.27 \pm 0.1).10^{-7}$	$(7.3 \pm 0.7).10^{-7}$	$(1.5 \pm 0.2).10^{-7}$
2.5 m 2MPZ in water + NMP (1:1)				
0.30	4.7 ± 0.3	$(5.8 \pm 0.6).10^{-7}$	$(2.9 \pm 0.3).10^{-6}$	$(7.2 \pm 0.9).10^{-7}$
0.35	11.0 ± 0.9	$(2.3 \pm 0.2).10^{-7}$	$(1.3 \pm 0.1).10^{-6}$	$(2.8 \pm 0.3).10^{-7}$
0.39	34 ± 3	$(7.8 \pm 0.8).10^{-8}$	$(6.0 \pm 0.6).10^{-7}$	$(9 \pm 1).10^{-8}$

A.3. Data for 3.5 m MDEA solvents

Table 6. Data obtained for MDEA-based water lean solvents in the WWC at 40 °C

α (mol CO_2/mol N)	p_{CO2} (kPa)	K_g (mol/m^2.s.Pa)	k_g (mol/m^2.s.Pa)	k_g' (mol/m^2.s.Pa)

3.5 m MDEA in water				
0.25	8.8 ± 0.6	$(4.8 \pm 0.5).10^{-8}$	$(1.6 \pm 0.2).10^{-6}$	$(5.0 \pm 0.5).10^{-8}$
0.30	13.5 ± 0.8	$(4.4 \pm 0.4).10^{-8}$	$(1.2 \pm 0.1).10^{-6}$	$(4.6 \pm 0.5).10^{-8}$
0.35	22 ± 9	$(1.6 \pm 0.2).10^{-8}$	$(1.0 \pm 0.1).10^{-6}$	$(1.6 \pm 0.2).10^{-8}$
3.5 m MDEA in water + SULF (1:1)				
0.10	9.4 ± 0.5	$(6.0 \pm 0.6).10^{-8}$	$(1.0 \pm 0.1).10^{-6}$	$(6.4 \pm 0.7).10^{-8}$
0.15	17 ± 2	$(5.1 \pm 0.5).10^{-8}$	$(1.0 \pm 0.1).10^{-6}$	$(5.3 \pm 0.6).10^{-8}$
0.20	30 ± 7	$(4.7 \pm 0.5).10^{-8}$	$(6.0 \pm 0.6).10^{-7}$	$(5.0 \pm 0.5).10^{-8}$
3.5 m MDEA in water + MEG (1:1)				
0.10	7.7 ± 0.7	$(5.5 \pm 0.5).10^{-8}$	$(1.0 \pm 0.1).10^{-6}$	$(5.8 \pm 0.6).10^{-8}$
0.15	13.6 ± 0.7	$(4.8 \pm 0.5).10^{-8}$	$(1.0 \pm 0.1).10^{-6}$	$(5.1 \pm 0.5).10^{-8}$
0.21	23 ± 3	$(2.7 \pm 0.3).10^{-8}$	$(7.3 \pm 0.7).10^{-7}$	$(2.8 \pm 0.3).10^{-8}$
3.5 m MDEA in water + 1MIMI (1:1)				
0.10	13.0 ± 0.7	$(6.8 \pm 0.7).10^{-8}$	$(1.0 \pm 0.1).10^{-6}$	$(7.3 \pm 0.8).10^{-8}$
0.15	22 ± 2	$(4.9 \pm 0.5).10^{-8}$	$(7.3 \pm 0.7).10^{-7}$	$(5.3 \pm 0.6).10^{-8}$
3.5 m MDEA in water + DMSO (1:1)				
0.10	17 ± 1	$(2.5 \pm 0.2).10^{-8}$	$(7.3 \pm 0.7).10^{-7}$	$(2.6 \pm 0.3).10^{-8}$
0.15	33 ± 4	$(2.2 \pm 0.2).10^{-8}$	$(6.0 \pm 0.6).10^{-7}$	$(2.3 \pm 0.2).10^{-8}$
3.5 m MDEA in water + NMP (1:1)				
0.10	24 ± 1	$(3.6 \pm 0.4).10^{-8}$	$(7.3 \pm 0.7).10^{-7}$	$(3.8 \pm 0.4).10^{-8}$

Appendix B. Obtaining the confidence intervals for p_{CO2} and k_g'

B.1. The uncertainty of the equilibrium CO_2 partial pressure

As mentioned before, the WWC is employed in both bypass and operational configurations. With these, and by operating them in absorption and desorption modes, one can gather a set of data as seen in Figure 8. In the desorption mode, the CO_2 partial pressure measured in bypass configuration is lower than that measured in operational configuration. The opposite happens in the absorption mode. If both had equal values, this would mean that the CO_2 partial pressure coming through the inlet stream was exactly the CO_2 partial pressure in equilibrium with the loaded solution. The key to obtaining this value, therefore, is the linear regression showed in blue.

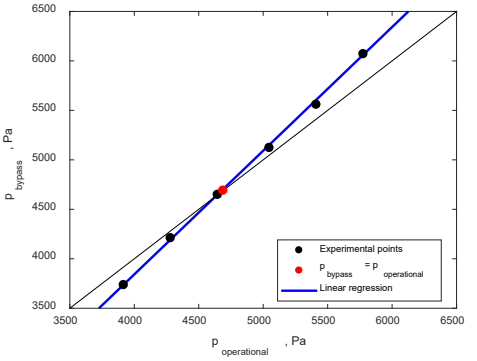

Fig. 8. Operational and bypass modes of the WWC being used for obtaining the CO_2 partial pressure

Two parameters are obtained in the linear regression, Eq. (12). The equilibrium CO_2 partial pressure can be calculated from these parameters by Eq. (13).

$$p_{bypass} = \beta_1 + \beta_2 \cdot p_{operational} \tag{12}$$

$$p_{CO2} = \frac{\beta_1}{1-\beta_2} \tag{13}$$

As p_{CO2} is not measured directly but is indeed evaluated with the parameters obtained by Eq. (12), its accuracy depends entirely on the quality of the fitting. Equation (14) shows how this can be done.

$$\left(\delta p_{CO2}\right)^2 = \left(\frac{p_{CO2}}{\beta_1}\right)^2 \cdot \left(\delta\beta_1\right)^2 + \left(\frac{p_{CO2}}{1-\beta_2}\right)^2 \cdot \left(\delta\beta_2\right)^2 \tag{14}$$

The variances of the slopes (β_2) and intercepts (β_1) of each regression line may be easily calculated with any statistics tool. In the end, the quality of the CO_2 partial pressure data obtained will depend on how many points are measured and how much they diverge from a straight line. Since with each measurement one may affect the loading of the solvent being analyzed, a compromise is required to obtain good results with not so many data points.

B.2. The uncertainty of the liquid phase mass transfer coefficient

As a rule of thumb, one can assume that K_g obtained in the WWC has an uncertainty of 10% and that the same is valid regarding k_g recovered from the empirical model (Bishnoi and Rochelle, 2000). Clearly, if both have the same confidence margins, then the confidence margin for k_g' can be given by Equation (15).

$$\left(\delta k_g'\right)^2 = \left[2 \cdot \left(\frac{k_g'^2}{K_g^2} - \frac{k_g'}{K_g}\right) + 1\right] \cdot \left(0.1 \cdot k_g'\right)^2 \tag{15}$$

Essentially, the uncertainty of k_g' is proportional to k_g' itself, reaching a minimum when k_g' = K_g, i.e. when gas-film mass transfer resistance is negligible and k_g is high. This is reasonable: if gas-film mass transfer resistance can be ignored, than the WWC procedure would be measuring k_g' directly. The estimated value of k_g decreases with high pressures and increases with vapor velocity (Bishnoi and Rochelle, 2000). Once again, these parameters are limited by the operational span of the apparatus and accuracy of the mass flow controllers. For solvents with very fast absorption rates, as was the case of some water lean solvents with MEA, it happened a few times that Equation (7) resulted in statistically insignificant k_g's values. These values were not included in this work.

References

Akhfash, M., Arjmandi, M., Aman, Z.M., Boxall, J.A., May, E.F., 2017. Gas Hydrate Thermodynamic Inhibition with MDEA for Reduced MEG Circulation. J. Chem. Eng. Data 62, 2578–2583. https://doi.org/10.1021/acs.jced.7b00072

Alvarez-Fuster, C., Midoux, N., Laurent, A., Charpentier, J.C., 1981. Chemical kinetics of the reaction of CO_2 with amines in pseudo m–nth order conditions in polar and viscous organic solutions. Chem. Eng. Sci. 36, 1513–1518. https://doi.org/10.1016/0009-2509(81)85112-3

Bara, 2011. US8506914B2 - N-functionalized imidazole-containing systems and methods of use. URL https://patents.google.com/patent/US8506914B2/en (accessed 11.27.18).

Bezuglaya, E.P., Lyapunov, N.A., Krasnoperova, A.P., Yukhno, G.D., Chernyi, A.V., 2009. Viscosity and thermodynamics of the viscous flow of the system water – N-methylpyrrolidone. Visn. Chark. Nacional. Univ. Ser. Chim. 870, 199-207.

Bhown, A.S., Freeman, B.C., 2011. Analysis and Status of Post-Combustion Carbon Dioxide Capture Technologies. Environ. Sci. Technol. 45, 8624–8632. https://doi.org/10.1021/es104291d

Bishnoi, S., Rochelle, G.T., 2000. Absorption of carbon dioxide into aqueous piperazine: reaction kinetics, mass transfer and solubility. Chem. Eng. Sci. 55, 5531–5543. https://doi.org/10.1016/S0009-2509(00)00182-2

Chen, X., Rochelle, G.T., 2013. Modeling of CO_2 Absorption Kinetics in Aqueous 2-Methylpiperazine. Ind. Eng. Chem. Res. 52, 4239–4248. https://doi.org/10.1021/ie3023737

Du, Y., Yuan, Y., Rochelle, G.T., 2016. Capacity and absorption rate of tertiary and hindered amines blended with piperazine for CO_2 capture. Chem. Eng. Sci. 155, 397–404. https://doi.org/10.1016/J.CES.2016.08.017

Dugas, R.E., 2009. Carbon dioxide absorption, desorption, and diffusion in aqueous piperazine and monoethanolamine. Ph.D. dissertation. URL https://repositories.lib.utexas.edu/handle/2152/7586 (accessed 11.27.18).

Hamborg, E.S., van Aken, C., Versteeg, G.F., 2010. The effect of aqueous organic solvents on the dissociation constants and thermodynamic properties of alkanolamines. Fluid Phase Equilib. 291, 32–39. https://doi.org/10.1016/J.FLUID.2009.12.007

Hamborg, E.S., Derks, P.W.J., van Elk, E.P., Versteeg, G.F., 2011. Carbon dioxide removal by alkanolamines in aqueous organic solvents. A method for enhancing the desorption process. Energy Procedia 4, 187–194. https://doi.org/10.1016/j.egypro.2011.01.040

Hansen, C.M., 2007. Hansen solubility parameters : a user's handbook. CRC Press.

IEA Bioenergy, 2016. Plant Lists - IEA Bioenergy Task 37. URL http://task37.ieabioenergy.com/plant-list.html (accessed 11.27.18).

Jassim, M.S., Rochelle, G.T., 2006. Innovative absorber/stripper configurations for CO_2 capture by aqueous monoethanolamine. Ind. Eng. Chem. Res. 45, 2465-2472. https://doi.org/10.1021/IE050547S

Kohl, A.L., Nielsen, R.B., 1997. Physical Solvents for Acid Gas Removal. In: Gas Purification. 1187–1237. https://doi.org/10.1016/B978-088415220-0/50014-8

Lail, M., Tanthana, J., Coleman, L., 2014. Non-Aqueous Solvent (NAS) CO_2 Capture Process. Energy Procedia 63, 580–594. https://doi.org/10.1016/J.EGYPRO.2014.11.063

Leites, I.L., 1998. Thermodynamics of CO_2 solubility in mixtures monoethanolamine with organic solvents and water and commercial experience of energy saving gas purification technology. Energy Convers. Manag. 39, 1665–1674. https://doi.org/10.1016/S0196-8904(98)00076-4

Li, L., Li, H., Namjoshi, O., Du, Y., Rochelle, G.T., 2013. Absorption rates and CO_2 solubility in new piperazine blends. Energy Procedia 37, 370–385. https://doi.org/10.1016/J.EGYPRO.2013.05.122

Liu, F.-H., Huang, K.-M., Wang, F., Jia, G.-Z., 2016. Dielectric properties of 1-methylimidazole at temperatures 298–336 K. Phys. Chem. Liq. 1–6. https://doi.org/10.1080/00319104.2015.1095641

Maryott, A.A., Smith, E.R., 1951. Table of dielectric constants of pure liquids. National Bureau of Standards circular AD-A278-956. URL https://apps.dtic.mil/dtic/tr/fulltext/u2/a278956.pdf (accessed 11.28.18).

NIST Chemistry WebBook. URL https://webbook.nist.gov/chemistry/ (accessed 11.28.18).

Płowaś, I., Świergiel, J., Jadżyn, J., 2013. Relative Static Permittivity of Dimethyl Sulfoxide + Water Mixtures. J. Chem. Eng. Data 58, 1741–1746. https://doi.org/10.1021/je400149j

Reynolds, J.A., Hough, J.M., 1957. Formulae for Dielectric Constant of Mixtures. Proc. Phys. Soc. Sect. B 70, 769–775. https://doi.org/10.1088/0370-1301/70/8/306

Rivas, O.R., Prausnitz, J.M., 1979. Sweetening of sour natural gases by mixed-solvent absorption: Solubilities of ethane, carbon dioxide, and hydrogen sulfide in mixtures of physical and chemical solvents. AIChE J. 25, 975–984. https://doi.org/10.1002/aic.690250608

Roberts, B.E., Mather, A.E., 1988. Solubility of CO_2 and H_2S in a mixed solvent. Chem. Eng. Commun. 72, 201–211. https://doi.org/10.1080/00986448808940017

Rochelle, G., Chen, E., Freeman, S., Van Wagener, D., Xu, Q., Voice, A., 2011. Aqueous piperazine as the new standard for CO_2 capture technology. Chem. Eng. J. 171, 725–733. https://doi.org/10.1016/J.CEJ.2011.02.011

Ryckebosch, E., Drouillon, M., Vervaeren, H., 2011. Techniques for transformation of biogas to biomethane. Biomass and Bioenergy 35, 1633–1645. https://doi.org/10.1016/J.BIOMBIOE.2011.02.033

Sada, E., Kumazawa, H., Han, Z.Q., Matsuyama, H., 1985. Chemical kinetics of the reaction of carbon dioxide with ethanolamines in nonaqueous solvents. AIChE J. 31, 1297–1303. https://doi.org/10.1002/aic.690310808

Sada, E., Kumazawa, H., Osawa, Y., Matsuura, M., Han, Z.Q., 1986. Reaction kinetics of carbon dioxide with amines in non-aqueous solvents. Chem. Eng. J. 33, 87–95. https://doi.org/10.1016/0300-9467(86)80038-7

Semenova, T.A., Leites, I.L., 1977. Purification of gases by solutions of alkanolamines in organic solvents. In: The purification of technological gases. 236-245.

Shannon, M.S., Bara, J.E., 2011. Properties of Alkylimidazoles as Solvents for CO_2 Capture and Comparisons to Imidazolium-Based Ionic Liquids. Ind. Eng. Chem. Res. 50, 8665–8677. https://doi.org/10.1021/ie200259h

Song, J.H., Park, S.B., Yoon, J.H., Lee, H., Lee, K.H., 1997. Solubility of Carbon Dioxide in Monoethanolamine + Ethylene Glycol + Water and Monoethanolamine + Poly(ethylene glycol) + Water at 333.2 K. https://doi.org/10.1021/JE960203W

Svensson, H., Hulteberg, C., Karlsson, H.T., 2014. Precipitation of AMP Carbamate in CO_2 Absorption Process. Energy Procedia 63, 750–757. https://doi.org/10.1016/J.EGYPRO.2014.11.083

Tilstam, U., 2012. Sulfolane: A Versatile Dipolar Aprotic Solvent. Org. Process Res. Dev. 16, 1273–1278. https://doi.org/10.1021/op300108w

TUV, 2012. Biogas to Biomethane Technology Review. Produced by Vienna University of Technology (Austria), Institute of Chemical Engineering. Research divison: Thermal Process Engineering and Simulation. As part of delivery: Promotion of bio-methane and its market development through local and regional partnerships. A project under the Intelligent Energy-Europe programme. Contract Number: IEE/10/130. Deliverable Reference: Task 3.1.1.

Versteeg, G.F., van Swaaij, W.P.M., 1988. On the kinetics between CO_2 and alkanolamines both in aqueous and non-aqueous solutions—I. Primary and secondary amines. Chem. Eng. Sci. 43, 573–585. https://doi.org/10.1016/0009-2509(88)87017-9

Woertz, B.B., 1972. Experiments with solvent-amine-water for removing CO_2 from gas. Can. J. Chem. Eng. 50, 425–427. https://doi.org/10.1002/cjce.5450500321

Wu, S., Yang, H., Hu, J., Shen, D., Zhang, H., Xiao, R., 2017. The miscibility of hydrogenated bio-oil with diesel and its applicability test in diesel engine: A surrogate (ethylene glycol) study. Fuel Process. Technol. 161, 162–168. https://doi.org/10.1016/J.FUPROC.2017.03.022

Yamamoto, S., Yamada, H., Higashii, T., 2014. Development of Chemical CO_2 Solvent For High Pressure CO_2 Capture (2): Addition Effects of Non-aqueous Media on Amine Solutions. Energy Procedia 63, 1963–1971. https://doi.org/10.1016/J.EGYPRO.2014.11.209

Yuan, Y., Rochelle, G.T., 2018. CO_2 absorption rate in semi-aqueous monoethanolamine. Chem. Eng. Sci. 182, 56–66. https://doi.org/10.1016/J.CES.2018.02.026

Yuan, Y., 2018. Mass transfer rate in semi-aqueous amines for CO_2 capture. Ph.D. dissertation.